Indian Journal of Chemistry
Vol. 54A, December 2015, pp. 1423-1433

Hydrogen sorption in phosphorous substituted carbon material

Arjunan Ariharan[a,b], Balasubramanian Viswanathan[a,] * & Vaiyapuri Nandhakumar[b]

[a]National Centre for Catalysis Research, Indian Institute of Technology Madras, Chennai, India
Email: bvnathan@iitm.ac.in

[b]PG & Research Department of Chemistry, AVVM Sri Pushpam College Poondi, Bharathidasan University, Trichirapalli 620 001, Tamilnadu, India

Received 6 October 2015; revised and accepted 20 November 2015

The hydrogen storage capacity of phosphorous substituted carbon material with spherical morphology is reported. The phosphorous substituted carbons are synthesized by pyrolyzing a resorcinol formaldehyde resin, chemically bonded with phosphorous. The synthesis is a polycondensation reaction by phosphoric acid with sodium hydroxide as catalyst. Herein resorcinol-formaldehyde resin and phosphoric acid act as carbon and phosphorous sources respectively. The hydrogen adsorption capacity has been studied by high pressure volumetric analyser and shows high sorption capacity of 2.6 and 2 wt% at 298 K and 100 bar pressure for the phosphorous substituted carbon materials prepared by calcining at 600 and 800 °C respectively. This value is higher than the hydrogen sorption capacity of pure carbon under comparable preparation conditions 0.18 and 0.16 wt% at 298 K and 100 bar pressure, calcined at 600 and 800 °C respectively.

Keywords: Hydrogen storage, Carbon materials, Heteroatom substituted carbon, Phosphorus substituted carbon, Carbonization, Hydrogen adsorption capacity.

Hydrogen storage is a crucial segment for the advancement of a hydrogen-based energy carrier in transport sector. Hydrogen is viewed as a future fuel and effective energy bearer, since its burning just produces water as byproduct. In this energy scene, generation and storage are the two key factors and identifying suitable materials for hydrogen generation and storage is a vital requirement. Nanostructured materials have of late received considerable attention as materials suitable for hydrogen storage[1-6]. The DOE has stipulated a hydrogen storage ability of 4.5 wt% by the FY 2005, 6.0 wt% by the FY 2010, and 9.0 wt% by the FY 2015 as the targets. However these targets could not be accomplished and these limits are being modified periodically. It has been understood that at least 6.25 wt% of hydrogen storage is essential for commercial exploitation. Right now, there are a several methodologies that are being tried for the storage of hydrogen. One approach is to upgrade the existing materials chemically, with the presumption that solid state storage is the only promising route. Variety of solid state hydrogen storage materials have been developed in the previous decades taking into account some criteria like storage capacity, reversibility and cost. Solid state hydrogen storage is attempted in solid substrates like metal–organic frameworks (MOFs) and their functionalized subsidiaries, chemical hydrides and covalent organic frameworks (COFs)[7-14]. Carbon-based materials have received extensive enthusiasm for many energy-related applications because of their chemical and thermal stability, and the feasibility to tune its textural characteristics so as to satisfy the required characteristics[15-22]. Carbonaceous materials like carbon nanotubes, fullerenes, graphene and nano-porous carbon have been examined for this particular application. Hydrogen storage in carbon materials received significant consideration after a storage capacity (though unexpectedly high) of around 67 wt% was reported in literature. Carbon materials for hydrogen storage must be related to the surface area with appropriate pore size[23]. Clearly carbon materials prepared from polymeric precursors have received an expanding consideration for their wide applications as adsorbents, electrode materials and catalyst supports because of the unprecedented properties, for example, low mass density, extensive porosity and high surface area[15, 24-27]. Hydrogen storage on carbon materials including carbon nanotubes (CNTs), graphite nanofibers (GNFs), activated carbons (ACs), template carbons (TCs) and graphite has been generally studied[27-38]. Current theoretical and experimental investigations have shown that the hydrogen binding energy and hydrogen adsorption ability of carbon

materials can be regulated by heteroatom substitution, for example by boron, phosphorous or nitrogen[39]. Systems and procedures have been developed to produce heteroatom substituted carbon materials in view of the low cost, energy and low toxicological effects[40]. By and large, the synthetic strategy for the heteroatom-substituted carbon materials is through carbonization of heteroatom and carbon containing precursors followed by a supplementary physicochemical activation[41]. Another way to generate heteroatom substituted carbon material is to post-treat carbon materials with suitable precursors like phosphoric acid[42-44]. The extend of doping depends on the antecedent and the aromatization level of preparatory carbonaceous materials[45]. In addition, the surface functionalities of the heteroatom substituted carbon materials depend on the carbonization temperature[46-49]. Heteroatom doping of carbon materials is a developing field of materials science. Rather, if heteroatoms similar to N, P, B and S are incorporated in carbon matrices, then these sites can work as hydrogen activating and dissociating centres and the dissociated hydrogen can be transported forward and backward on to the equipotential carbon surface[12, 46, 50-56]. Heteroatom substituted sites in carbon may function as activation centres for the activation and dissociation of molecular hydrogen and its transport to carbon centres for storage and in a similar manner these centres can also act for the desorption of hydrogen. As one of the available possibilities, phosphorous substitution in carbon materials can be examined for hydrogen storage applications[39, 57]. The present study is an attempt in this direction.

Phosphorous substituted carbon materials has been synthesized using resorcinol and phosphoric acid as carbon and phosphorous sources respectively. The structural, chemical, morphological and textural characteristics of the synthesized materials have been examined by powder X-ray diffraction patterns (PXRD), Fourier transform infrared spectroscopy (FT-IR), Confocal Raman spectroscopy, BET-N_2 adsorption/desorption isotherms, high resolution scanning electron microscopy (HRSEM), high resolution Transmission electron microscopy (HRTEM), and X-ray photoelectron spectroscopy (XPS). The hydrogen storage capacity of the phosphorous substituted carbon material has been determined by high pressure volumetric analyzer (HPVA 100).

Materials and Methods

Resorcinol 99% ($C_6H_6O_2$), formaldehyde 37% (HCHO) solution, sodium hydroxide 97% (NaOH) and phosphoric acid 88% (H_3PO_4) were purchased from Sigma Aldrich and used without further purification.

Schematic illustration of the synthesis of phosphorous substituted carbon material is shown in Fig. 1. The typical synthesis procedure is as follows: 5.5 g of resorcinol was taken in a beaker, and 15 mL of formaldehyde solution was added, stirred at room temperature for 1 h and then 31 mL of phosphoric acid (H_3PO_4) was added stirred for 1 h followed by 1 g of sodium hydroxide (NaOH) stirred well at room temperature, then kept in an oven at 373 K for 24 h. The final homogeneous mixture was placed in a quartz boat and subsequently transferred to a tube furnace for carbonization. The furnace was purged with nitrogen gas at room temperature for 1 h. Then the temperature was increased at a rate of 5 °C/min up to 300 °C and maintained at 300 °C for 5 min to remove traces of adsorbed contaminants. After 5 min, the temperature was increased at a rate of 5 °C/min to

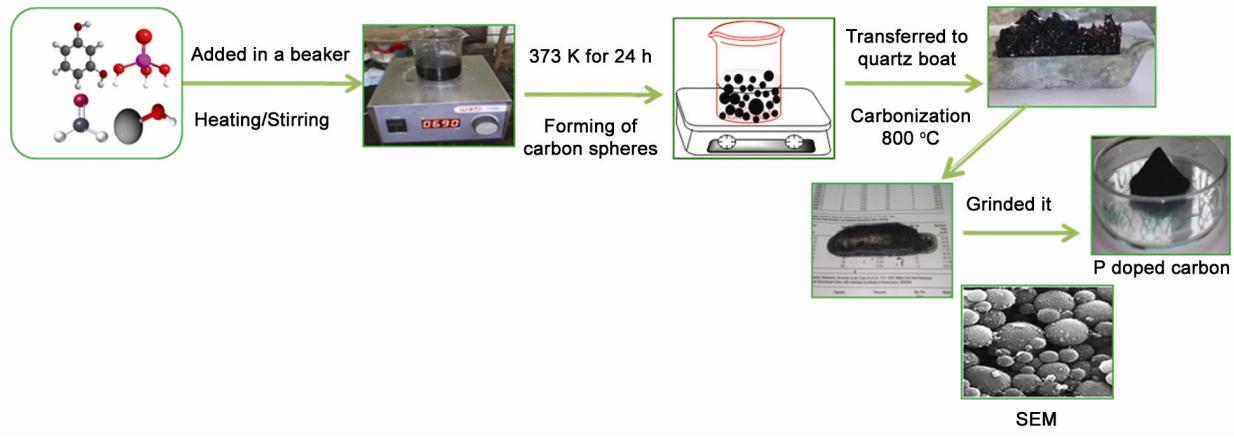

Fig. 1—The schematic illustration of the synthesis of phosphorous substituted carbon material.

the target temperature (600 and 800 °C). Upon reaching the target temperature, the temperature was maintained an additional 6 h. The furnace was cooled to room temperature in the presence of nitrogen. Throughout the procedure, the furnace was continually purged with nitrogen gas. The resulting carbon material was ground into a fine powder using a mortar and pestle. Finally the obtained phosphorous containing carbon material was subjected to further characterization. A similar synthesis procedure was adopted to prepare pure carbon material without phosphorous for comparison purpose.

Characterisation

Wide angle powder XRD pattern of the calcined carbon materials was recorded using a Rigaku Miniflex II diffractometer with CuKα as the radiation source at a wavelength of 0.154 nm with 2θ angle ranging from 10° to 80° with a step size of 0.02°. Fourier transform infrared spectra (Perkin-Elmer FTIR spectrophotometer) were collected at room temperature by using the KBr pellet technique working in the range of wave numbers 4000–400 cm^{-1}. The vibrational characteristics of the samples were analyzed via Raman spectroscopy using 532 nm laser (Witec Alpha 300) as the excitation source in the range from 1000 to 2000 cm^{-1}. N_2 adsorption and desorption isotherms were measured with surface area and porosity analyzer Micromeritics accelerated surface area and porosimetry system (ASAP 2020) for the determination of surface area and total pore volume at 77 K. Prior to the adsorption measurements, the sample was degassed at 473 K for 6 h. FEI Quanta FEG 200-high resolution scanning electron microscope (HRSEM) was employed for obtaining the micrographs. AJEOL JEM-2100 high resolution transmission electron microscope (HRTEM) was employed for obtaining the micrographs, Elemental mapping and SAED patterns. X-ray photoelectron spectroscopy (XPS) measurements were performed with an Omicron nanotechnology spectrometer with hemispherical analyzer. The monochromatized Mg Kα X-source (E = 1253.6 eV) was operated at 15 kV and 20 mA. For the narrow scans, the analyzer pass energy of 25 eV was employed. The base pressure in the analysis chamber was 5×10^{-10} Torr. The hydrogen adsorption isotherms were carried out on high pressure volumetric analyzer (HPVA-100) from micromeritics particulate systems. The HPVA product operating pressure ranges from high vacuum to 100 bar. The span of the sample temperature during analysis can be from cryogenic to 500 °C. Sample analysis data collection is fully automated to assure quality data and high reproducibility.

Hydrogen adsorption measurements

High pressure hydrogen adsorption measurements have been carried out utilizing high pressure volumetric analyzer (HPVA 100). The high pressure adsorption analyzer comprises a cylindrical sample cell of known volume (2 cc and 10 cc). Utmost care was taken with respect to the sources of leak and long blank run tests were carried out. Care was also taken to avoid temperature instability, leaks and additional pressure and temperature impacts caused by expansion of the hydrogen in the sample cell. The isotherms were completed as accurately as possible. Typically, the mass of the carbon samples used for hydrogen storage measurements was in the region of 500 mg to 1 g. Prior to measurement, the samples were degassed and heated at 250 °C for approximately 6 h in vacuum. The whole system was pressurized at the desired value by hydrogen and change in pressure was monitored. All the hydrogen adsorption isotherms were recorded at room temperature and liquid N_2 temperature. The trials were repeated under the same conditions for repeatability.

Results and Discussion

X-ray diffraction patterns

The X-ray diffraction pattern of the acquired phosphorous containing carbon material is shown in Fig. 2. The carbon samples prepared at 600 and 800 °C show wide diffraction reflections at 2θ values at 24°. This reflection is assigned to the (002) plane of

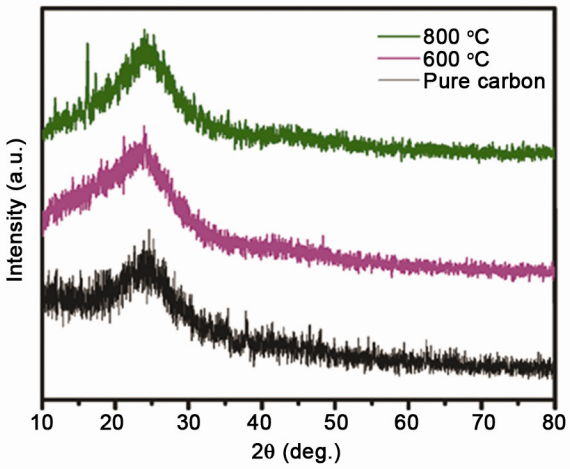

Fig. 2—XRD patterns of the phosphorous substituted carbon material.

the regular turbostratic carbon lattice. No other reflections are seen, showing the absence of any impurity in the material prepared[58]. This is further confirmed by the HRTEM-SAED patterns of prepared material (vide infra). The (100) reflection indicates the amorphous nature of the sample. The shifts towards the higher angles of the (002) at higher temperature shows an increase in the interlayer spacing. This increment in the *d*-spacing is identified with the doping of heteroatom. Since the amount of phosphorus is small, changes in 2θ values are not effectively noticeable despite the fact that the peaks are slightly shifted to higher 2θ values. The presence of heteroatom i.e., phosphorous (P) in the carbon lattice leads to defects and disorder[59, 60]. This is confirmed by the Raman spectrum of the material discussed later. It is reasoned that the carbon material is most likely less crystalline in nature.

FT-IR spectroscopy

FT-IR spectrum of the phosphorous substituted carbon material is shown in Fig. 3. The spectrum shows a broad absorption band in the region of 3200–3600 cm^{-1}. This band can be assigned to the O-H stretching mode of vibration of adsorbed water and hydroxyl groups. The position and the symmetry can be interpreted as due to internal hydrogen bonding. The band at 1600–1650 cm^{-1} is attributed to C–O stretching and C–OH bending modes. The band at 1636 cm^{-1} may be because of the aromatic ring stretching vibrations. The broad band in the region 1120–1170 cm^{-1} attributed to P–O–C and stretching of P=O groups stretching vibrations and a band at 1050 cm^{-1} is related to the symmetric vibration of P–O–P[61]. The absorption components at 2926 and 2850 cm^{-1} may be due to the aliphatic character of the C–H bonds. The absorption components at 2330, 1750 and 1018 cm^{-1} with shoulders are connected with C–P bonds. Similar observations have been recorded by Puziy *et al*[62] Kurita *et al.*[63] These observations reveal the presence of P in the carbon framework.

Raman spectroscopy

Raman spectrum of the phosphorous containing carbon material is shown in Fig. 4. The spectrum of the phosphorous containing carbon material showed two broad peaks around 1325 cm^{-1} and 1602 cm^{-1} usually designated as D and G bands[64]. These two bands showed the presence of defects and graphitic nature of the carbon material. The D-band brought about by structural defects and the mostly disordered structure of sp^2 hybridized carbon, and the G-band connected with the first-order scattering of the E_{2g} vibrations observed for sp^2 hybridized carbon[65]. The relative intensities (I_D/I_G) of these peaks depend on the carbonization degree and heteroatom substitution in the carbon materials. The ratio of integrated intensity (I_D/I_G) of the D and G bands computed for these materials can be utilized to estimate the defects in carbon material. It is found that I_D/I_G value for phosphorous containing carbon prepared at 800 °C = 1.29 and that for carbon material prepared at 600 °C is = 1.04. For the pure carbon material this intensity ratio I_D/I_G is 0.85. Phosphorous containing carbon material prepared at 800 °C is having higher intensity ratio value (1.29) contrasted to carbon material prepared at 600 °C (1.04) these values demonstrate higher concentration of structural defects in the phosphorous containing carbon material. Moreover, the intensity ratio of D and G band (I_D/I_G) in both

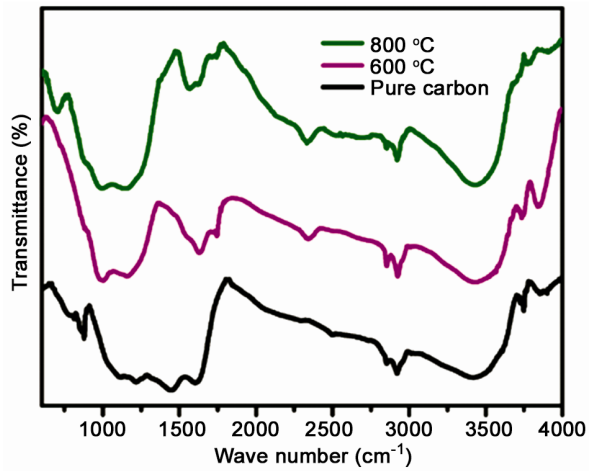

Fig. 3—FTIR spectra of the phosphorous substituted carbon material.

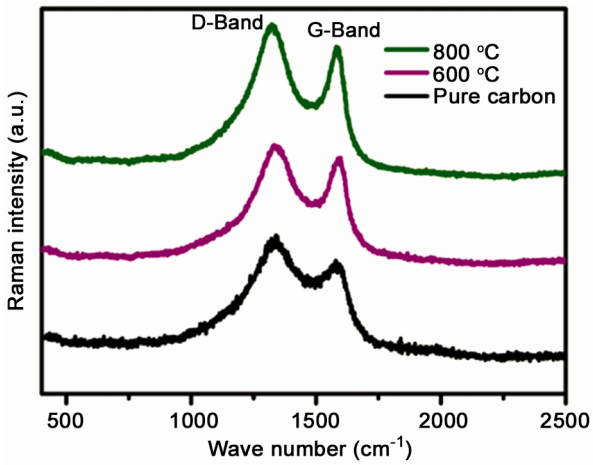

Fig. 4—Raman spectra of the phosphorous substituted carbon material.

carbon materials prepared at 600 °C and 800 °C is observed to be higher than for the pure carbon, suggesting that the degree of disorder increases after P substitution. Two differences in the I_D/I_G ratio show that the carbon structure turns out to be more disordered with increasing carbonization temperature[59,66].

N_2 adsorption/desorption isotherm

Brunauer-Emmett-Teller (BET) and Barret-Joyner-Halenda (BJH) methods are utilized to compute the specific surface area and pore size distribution of the phosphorous substituted carbon materials and the outcomes are shown in Fig. 5. N_2 adsorption isotherm is done on this material in the wake of degassing at 200 °C for 4 hours. The nitrogen adsorption isotherms of carbon samples prepared at 600 and 800 °C (Fig. 5a) are comparable to type IV isotherm as per the characterization of the International Union of Pure and Applied Chemistry (IUPAC). The presence of a H4 hysteresis loop shows the presence of both micropores and mesopores. Furthermore H4 hysteresis loop indicates the presence of narrow slit type pores. The isotherms show a steep uptake at P/P_0 = 0.15, and a hysteresis loop from P/P_0 = 0.4 to P/P_0 = 1.0 which is due to the co-existence of both micropores and mesopores[67]. Furthermore, the pore size analysis established the porous characteristic of the prepared material. The pore volume data (Supplementary Data, Table S1) show that the phosphorous containing carbon has a higher pore volume than the pure carbon material. The pore size distribution curves shown in Fig. 5(b), computed according to the Barrett-Joyner-Halenda (BJH) model, reveal that the majority of the pores in the prepared carbon materials have size below 5 nm. It may be noted that regardless of the presence of a large number of mesopores and micropores in the prepared material, the total pore volume for carbon prepared at 800 °C (0.095 cm^3/g) is higher as compared to carbon prepared at 600 °C (0.051cm^3/g). The mesopores correspond to the interparticle cavities resulting from the stacking of carbon spheres. Carbon prepared at 800 °C demonstrates a steady adsorption curve as the pressure increases with limited hysteresis loop, suggesting the presence of micropores. As the carbonization temperature increases, clear hysteresis loop profile alongside expansion in the adsorption curve at higher pressure is observed. In this phosphorous substituted carbon material when the carbonization temperature is increased the surface area, pore volume and micropore area are increased slightly. The specific surface area of carbon materials prepared at 600 °C and 800 °C is 35 and 82 m^2/g respectively. These data are summarised in Table S1 (Supplementary Data).

High resolution scanning electron microscopy (HRSEM)

The morphological aspects of the phosphorous containing carbon materials have been examined by the scanning electron micrographs and are shown in Fig. 6. These carbon materials show spherical morphology as seen from the micrographs. Besides it is conceivable that a greater part of the heteroatom (P) may be segregating on the surface, and thus, facilitating hydrogen activation. The spherical morphology may have been induced by the chemical activation with H_3PO_4. Due to the phosphoric acid, large portions of the spherical carbon particles shrink, retaining the morphology. The corresponding

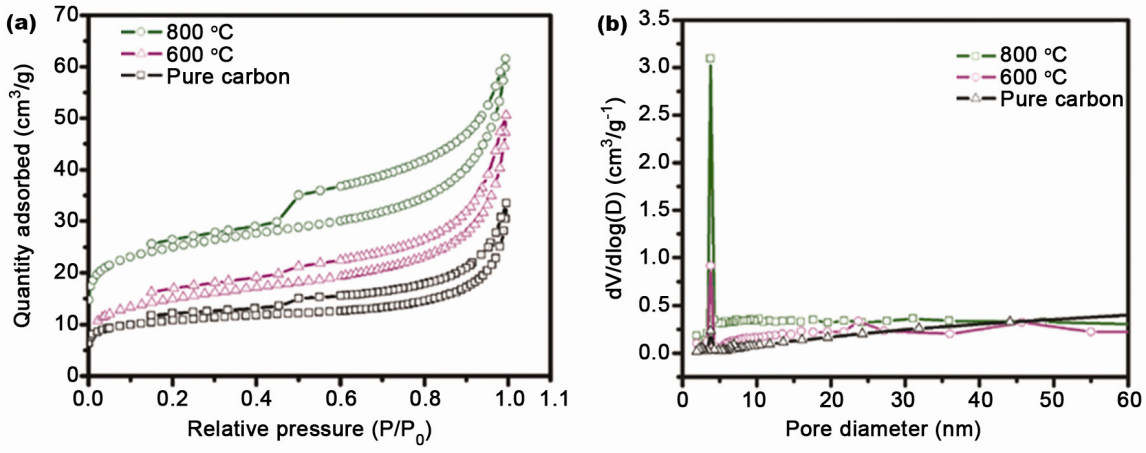

Fig. 5—(a) N_2 adsorption/desorption isotherm, and, (b) pore size distribution of the phosphorous substituted carbon material.

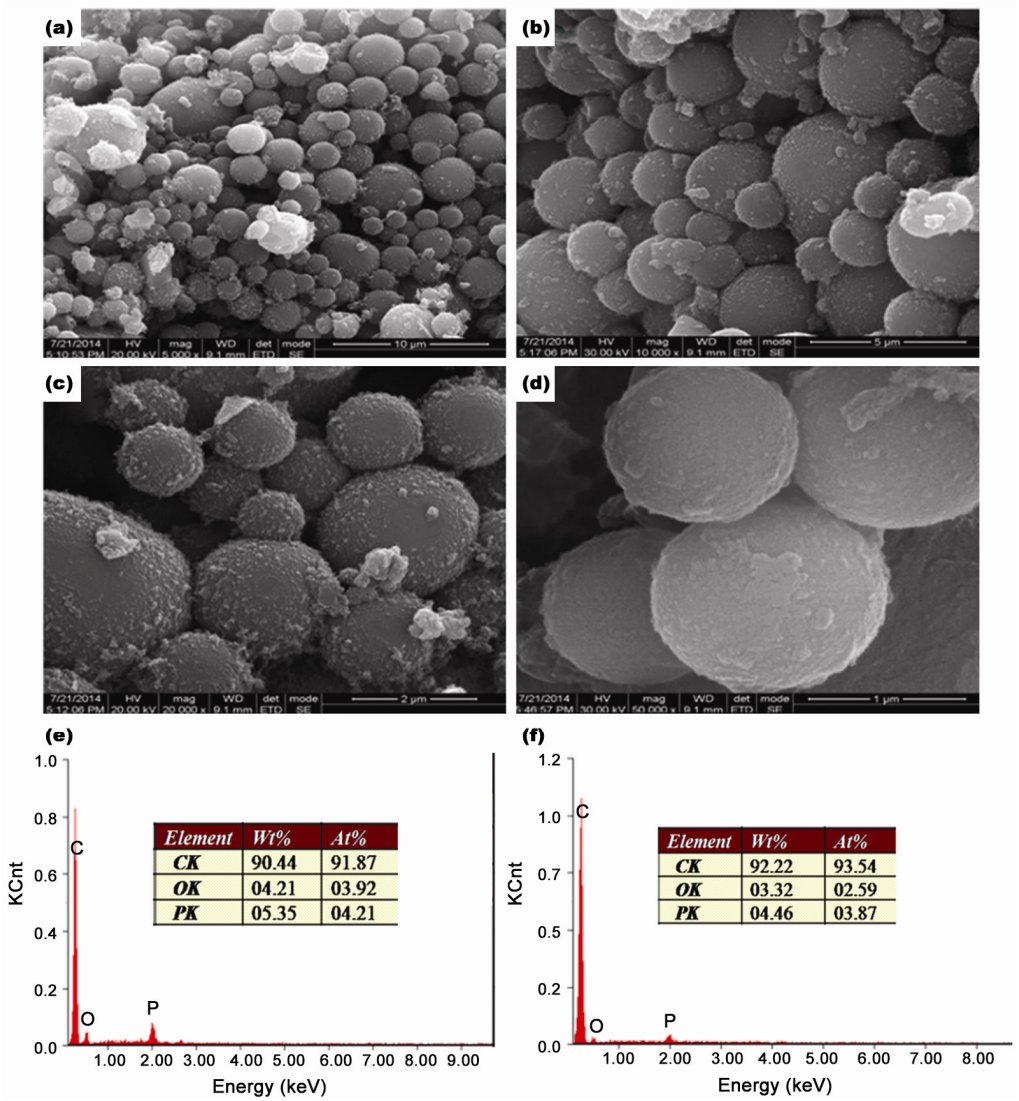

Fig. 6—(a, b, c and d) HRSEM images of the phosphorous substituted carbon material (prepared at 800 °C) for different magnifications, and, (e and f) SEM EDAX spectra for the phosphorous substituted carbon material.

situation in pure carbon materials is seen with sharp edges (see Supplementary Data, Figs S1 and S2). SEM EDAX analysis showed the amount of phosphorus in the carbon matrix to be 4 atomic percent (see Fig. 6(e, f)).

High resolution transmission electron microscopy (HRTEM)

The high resolution transmission electron micrographs and SAED patterns of the phosphorous containing carbon material are shown in Fig. 7. HRTEM micrographs show hollow spherical morphology of the prepared material. The selected area electron diffraction (SAED) pattern (Fig. 7(d)) shows two diffraction rings, indicating 002 and 100 planes and the disordered nature of the phosphorous substituted carbon material. Scanning TEM (STEM) with elemental mapping has been carried out to confirm the phosphorous substitution in the carbon lattice and to characterize the uniformity of substitution (see Fig. 7(e, f, g, h)) These results indicate carbon, phosphorus, and oxygen atoms distributed in the entire sample homogeneously. To explore the percentage of element, the TEM–EDAX investigation was carried out. The amount of phosphorous observed in the carbon matrix was ~4 at%. Moreover, since this reaction is completed in open atmosphere, some amount of oxygen is available in the carbon sample. The elemental composition monitored to evaluate the changes as a function of carbonization temperature are summarized in Table S2 (Supplementary Data).

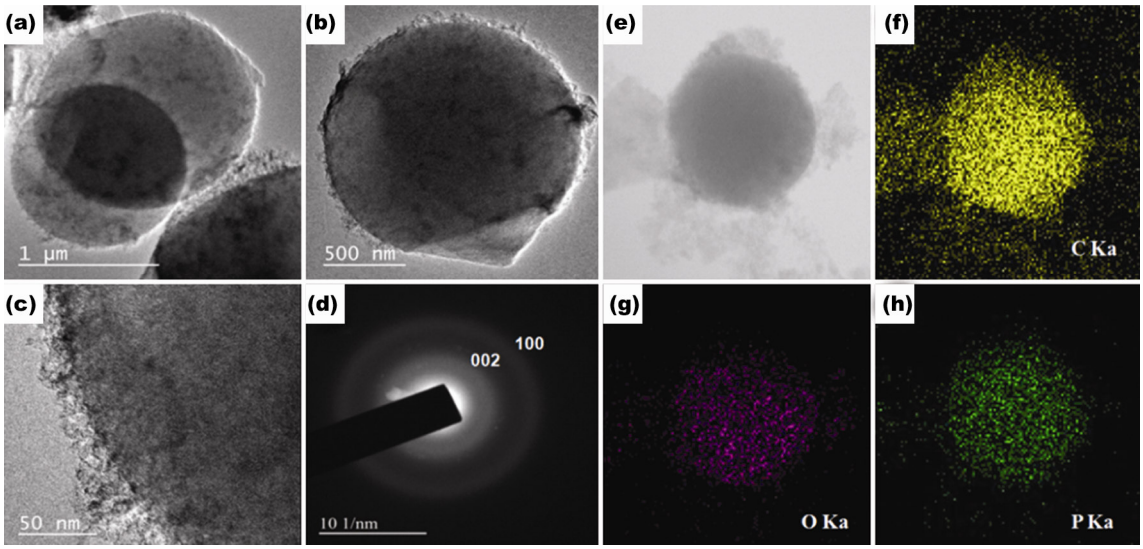

Fig. 7—(a, b, c) HRTEM images, (d) SAED pattern, (e) STEM image, and, (f, g, h) elemental mapping of the phosphorous substituted carbon material (prepared at 800 °C).

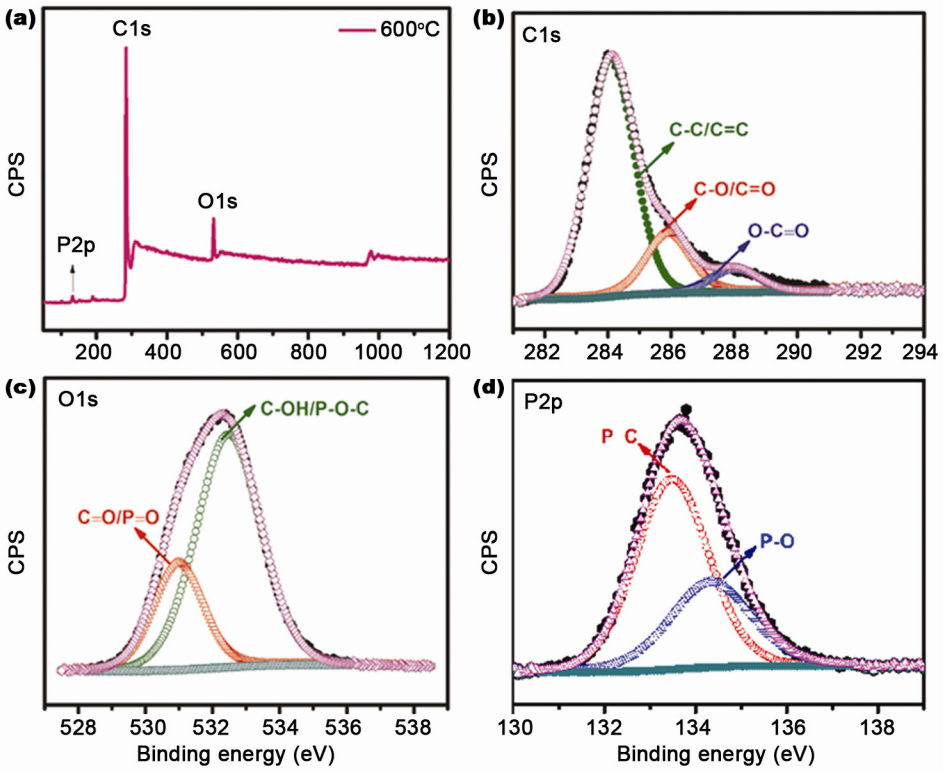

Fig. 8—X-ray photoelectron spectroscopy of the phosphorous substituted carbon material. [(a) XPS-survey spectrum; (b) C 1*s*; (c) P 2*p*; (d) O 1*s* (carbon prepared at 600 °C)].

X-ray photoelectron spectroscopy (XPS)

The chemical state of the substituted phosphorous in the carbon materials has been studied by X-ray photoelectron spectroscopy (XPS) and the spectra are given in Figs 8 and 9. The carbon species show standard 1*s* peaks at 284.3eV for sp^2-hybridized carbon bonds (C=C), 284.2 eV for sp^3-hybridized carbon bonds (C–C), 285.2 eV for alcohol groups (C–O), carbonyl groups (C=O), 289.2 eV for carboxylic/ester groups (O–C=O) (see Fig 8b). The oxygen species (Fig. 8c) are shown by 1*s* peak at binding energies ~531.1, 530.4, and 532.6 eV that

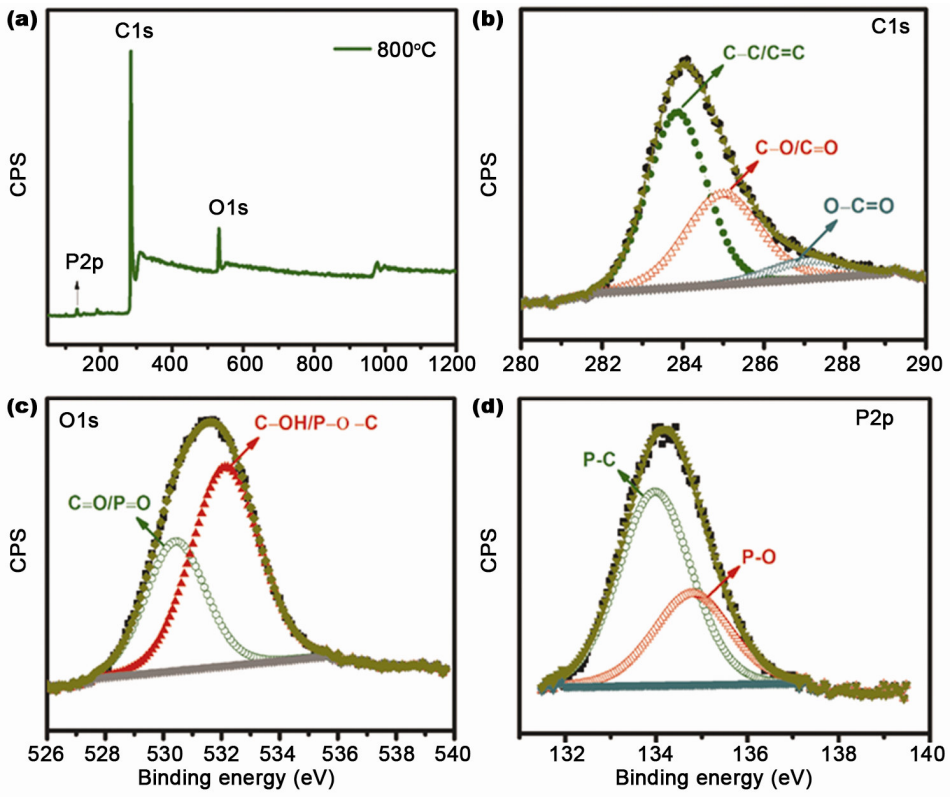

Fig. 9—X-ray photoelectron spectroscopy of the phosphorous substituted carbon material. [(a) XPS-survey spectrum; (b) C 1*s*; (c) P 2*p*; (d) O 1*s* (carbon prepared at 800 °C)].

correspond to C=O or P=O, C–OH or P–O–C groups and chemisorbed oxygen (carboxylic groups COOH) and/or water groups. The presence of P in the carbon material could be seen from the binding energy (BE) peak around 134.1 eV. Heteroatom forms covalent bond with the adjacent carbon in the carbon lattice. The deconvoluted *P* 2*p* peaks for the synthesized phosphorous substituted carbon material (see Fig. 8d) at 133.9eV and 134.5 eV can be assigned to P–C and P–O bonds[29,68,69]. The concentration of oxygen and phosphorous functionalities is temperature dependent. In general, at higher temperature, lower oxygen (phosphorous) functionalities is expected[59,62,70]. At a low temperatures (less than 500 °C), oxygen is bound to the carbonaceous matrix, and decreasing of O/P atomic ratio is attributed to the dehydrating effect of phosphoric acid. The carbon prepared at 800 °C shows more of all the similar binding energy peaks compared to the carbon prepared at 600 °C (see Fig. 9). Furthermore, the phosphorous level is decreased with increase of temperature (see Fig. 9(a, d)). However, the proportion of oxygen species that is bound to phosphorous increases significantly, when increasing the carbonization temperature (600–800 °C). Furthermore, oxygen is also present in small amounts due to reaction being carried out in open atmosphere. Indeed, the amount of heteroatom substitution depends on the category of precursors and the microscopic surface chemistry. The surface groups like hydroxyl groups facilitates heteroatom substitution[45]. The XPS measurements confirmed the substitution of phosphorous in the carbon matrix[42,71-77]. The elemental compositions monitored to evaluate the changes in the chemical composition as a function of carbonization temperature are summarized in Table S2 (Supplementary Data).

Hydrogen adsorption

The hydrogen adsorption isotherms on the prepared carbon material are given in Figs 10 and 11. It is seen that storage capacity of phosphorous containing carbon material prepared at 600 °C is 2.6 wt% while the carbon prepared at 800 °C showed sorption capacity of 2 wt% at 298 K and 100 bar pressure (Fig. 9). Phosphorous containing carbon material prepared at 600 °C and the carbon prepared at 800 °C showed sorption capacity of 0.28 wt% and 0.26 wt% at 77 K and 100 bar pressure (Fig. 10). The carbon

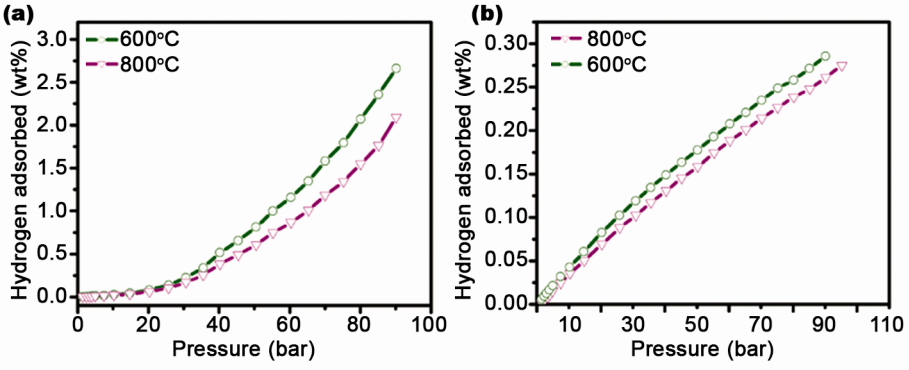

Fig. 10—Hydrogen adsorption isotherm of the phosphorous substituted carbon material prepared at 600 °C and 800 °C. [(a) 298 K; (b) 77 K and 100 bar pressure].

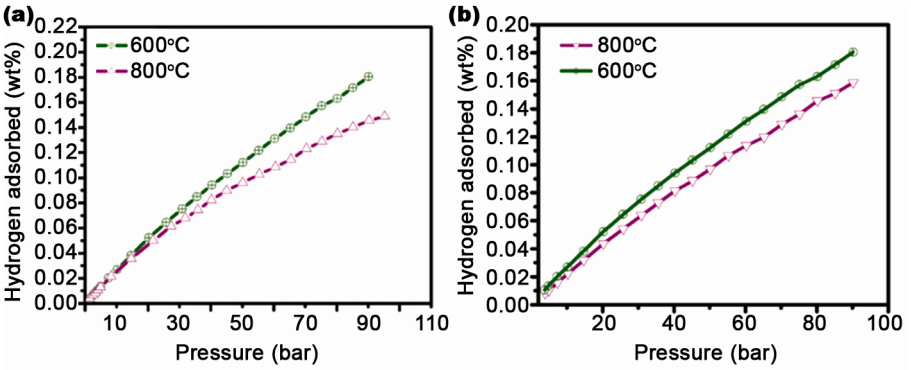

Fig. 11—Hydrogen adsorption isotherm of the pure carbon material (without P) prepared at 600 °C and 800 °C. [(a) 298K; (b) 77 K and 100 bar pressure].

materials without phosphorus substitution (at 600 and 800 °C) showed a storage capacity of 0.19 and 0.15 wt% respectively at 298 K and 100 bar pressure (Fig. 11). The carbon materials without phosphorus substitution (600 and 800 °C) showed a storage capacity of 0.18 and 0.14 wt% at 77 K and 100 bar pressure respectively (Fig. 11) (Supplementary Data, Table S3). The hydrogen storage capacity decreases with increase in temperature. These results can be considered as fillows: the hydrogen storage in these materials is by a process of adsorption and heteroatom substitution increases the storage capacity and nearly almost all the adsorbed amount can be desorbed with slight increase in temperature which is a desirable characteristic for hydrogen storage materials. In this case, the heteroatom (P) substitution provides appropriate centres for the dissociation of molecular hydrogen. Since heteroatoms take up substitution positions in the lattice, there is facile transport of hydrogen atoms on to the carbon surface. It is possible that most of the heteroatoms (P) may be segregating to the surface, thus facilitating hydrogen dissociation.

Conclusions

In summary, a preparation procedure for phosphorous substituted carbon materials has been developed. Phosphorous containing carbon materials produced by using polymer as the carbon precursor showed different chemical environments for phosphorous. The phosphorus substituted carbon materials calcined at 600 and 800 °C showed respectively 2.6 wt% and 2 wt% of hydrogen storage capacity at 298 K and 100 bar pressure. Phosphorous containing carbon material prepared at 600 °C and the carbon prepared at 800 °C showed sorption capacity of 0.28 wt% and 0.26 wt% at 77 K and 100 bar pressure. The pure carbon material prepared using the same sources and calcined at the same temperatures showed a storage capacity of 0.18 and 0.16 wt% at 298 K and 100 bar pressure. The hydrogen storage capacity decreases with increase in carbonization temperature. The results provide some insights into further increasing the hydrogen storage capacity in carbon materials and improving the reversibility. The discovery of excellent room temperature hydrogen

sorption materials such as heteroatom (P) substituted carbon is likely to motivate the search for increasing the extent of heteroatom substitution in carbon materials for improving hydrogen storage capacities. The simple and appealing strategy can easily be extended to the synthesis of other substituted carbon materials with tunable texture, surface and adsorption properties.

Acknowledgement

The authors wish to record their grateful thanks to the Department of Science and Technology (DST), New Delhi, India for supporting the National Centre for Catalysis Research, IIT Madras, Chennai, India, and, Ministry New and Renewable Energy, Govt of India, New Delhi, India, for supporting the hydrogen storage activity of this centre.

Supplementary Data

Supplementary data associated with this article, i.e., Fig. S1 (HRSEM images of the pure (without P) carbon material), Fig. S2 (HRSEM images of the phosphorous substituted carbon material prepared at 600 °C), Table S1 (BET-N_2 adsorption/desorption isotherm data for the phosphorous substituted carbon material), Table S2 (elemental composition of the phosphorous substituted carbon material measured by (i) SEM-EDAX, (ii) TEM-EDAX and (iii) XPS), and Table S3 (hydrogen adsorption isotherm results of the phosphorous substituted carbon and pure carbon material) are available in the electronic form at http://www.niscair.res.in/jinfo/ijca/IJCA_54A(12)1423-1433_SupplData.pdf.

References

1 Dillon A C, Jones K M, Bekkedahl T A, Kiang C H, Bethune D S & Heben M J, *Nature*, 386 (1997) 377.
2 Liu C, Fan Y Y, Liu M, Cong H T, Cheng H M & Dresselhaus M S, *Science*, 286 (1999) 1127.
3 Xia Y, Yang Z & Zhu Y, *J Mater Chem A*, 1 (2013) 9365.
4 Chambers A, Park C, Baker R T K & Rodriguez N M, *J Phys Chem B* 102 (1998) 4253.
5 Dalebrook A F, Gan W, Grasemann M, Moret S & Laurenczy G, *Chem Comm*, 49 (2013) 8735.
6 Konwar R J & De M, *Int J Energy Res*, 39 (2015) 223.
7 Yaghi O M, O'Keeffe M, Ockwig N W, Chae H K, Eddaoudi M & Kim J, *Nature*, 423 (2003) 705.
8 Kaye S S, Dailly A, Yaghi O M & Long J R, *J Am Chem Soc*, 129 (2007) 14176.
9 Zhao Y, Kim Y H, Dillon A C, Heben M J & Zhang S B, *Phys Rev Lett*, 94 (2005) 155504.
10 Ströbel R, Garche J, Moseley P T, Jörissen L & Wolf G, *J Power Sources,*159 (2006) 781.
11 He Z, Wang S, Wang X & Iqbal Z, *Int J Energy Res*, 37 (2013) 754.
12 Moussa G, Moury R, Demirci U B, Şener T & Miele P, *Int J Energy Res*, 37 (2013) 825.
13 Choma J, Osuchowski L, Marszewski M & Jaroniec M, *RSC Advances*, 4 (2014) 14795.
14 Musyoka N M, Ren J, Langmi H W, Rogers D E C, North B C, Mathe M & Bessarabov D, *Int J Energy Res*, 39 (2015) 494.
15 Sevilla M & Mokaya R, *Energy Environ Sci*, 7 (2014) 1250.
16 Candelaria S L, Shao Y, Zhou W, Li X, Xiao J, Zhang J G, Wong Y, Liu J, Li J & Cao G, *Nano Energy*, 1 (2012) 195.
17 Hynek S, Fuller W & Bentley J, *Int J Hydrog Energy*, 22 (1997) 601.
18 Su D S & Centi G, *J Energy Chem*, 22 (2013) 151.
19 Maria M T, Robin J W, Nicolas B, Vitaliy L B, Dang S S, Francisco D M, James H C & Mark J M, *Chem Soc Rev*, 44 (2015) 250.
20 Rao C N R , Urmimala M, Subrahmanyam K S, Gopalakrishnan K, Nitesh Kumar, Ram Kumar & Govindaraj A, *Indian J Chem,* 51A (2012) 31.
21 Sankaran M & Viswanathan B, *Indian J Chem,* 47A (2008) 814.
22 Chakraborty A, Duley S & Chattaraj P K, *Indian J Chem,* 51A (2012) 244.
23 Texier-Mandoki N, Dentzer J, Piquero T, Saadallah S, David P & Vix-Guterl C, *Carbon*, 42 (2004) 2744.
24 Tylianakis E, Klontzas E & Froudakis G E, *Nanoscale*, 3 (2011) 856.
25 Zhang Q, Uchaker E, Candelaria S L & Cao G, *Chem Soc Rev*, 42 (2013) 3127.
26 Kiciński W & Dziura A, *Carbon, 75* (2014) 56.
27 Zhu Y, Hu H, Li W & Zhang X, *Carbon*, 45 (2007) 160.
28 Pekala R W, Alviso C T, Kong F M & Hulsey S S, *J Non-Cryst, Solids*, 145 (1992) 90.
29 Jin H, Lee YS & Hong I, *Catal Today*, 120 (2007) 399.
30 Yang S J, Jung H, Kim T & Park C R, *Prog Nat Sci: Mater Int*, 22 (2012) 631.
31 Germain J, Fréchet J M J & Svec F, *Small*, 5 (2009) 1098.
32 Rzepka M, Lamp P & de la Casa-Lillo M A, *J Phys Chem B*, 102 (1998) 10894.
33 Bhatia S K, & Myers A L, *Langmuir*, 22 (2006) 1688.
34 Yang Z, Xia Y & Mokaya R, *J Am Chem Soc*, 129 (2007) 1673.
35 Nishihara H, Hou P X, Li L X, Ito M, Uchiyama M, Kaburagi T, Ikura A, Katamura J, Kawarada T, Mizuuchi K & Kyotani T, *J Phys Chem C*, 113 (2009) 3189.
36 Lee S Y & Park S J, *J Colloid Interface Sci*, 384 (2012) 116.
37 Stadie N P, Vajo J J, Cumberland R W, Wilson A A, Ahn C C & Fultz B, *Langmuir*, 28 (2012) 10057.
38 Marella M & Tomaselli M, *Carbon*, 44 (2006) 1404.
39 Blackman J M, Patrick J W, Arenillas A, Shi W & Snape C E, *Carbon*, 44 (2006) 1376.
40 Paraknowitsch J P & Thomas A, *Energy Environ Sci, 6* (2013) 2839.
41 Hu B, Wang K, Wu L, Yu S H, Antonietti M & Titirici M M, *Adv Mater*, 22 (2010) 813.
42 László K, Tombácz E & Josepovits K, *Carbon*, 39 (2001) 1217.

43 Hulicova-Jurcakova D, Puziy A M, Poddubnaya O I, Suárez-García F, Tascón J M D & Lu G Q, *J Am Chem Soc*, 131 (2009) 5026.

44 Villar-Rodil S, Suárez-García F, Paredes J I, Martínez-Alonso A & Tascón J M D, *Chem Mater*, 17 (2005) 5893.

45 Vázquez-Santos M B, Suárez-García F, Martínez-Alonso A & Tascón J M D, *Langmuir*, 28 (2012) 5850.

46 Zhu Y P, Liu Y, Liu Y P, Ren T Z, Chen T & Yuan Z Y, *Chem Cat Chem*, 7 (2015) 2909.

47 Wang C, Zhou Y, Sun L, Wan P, Zhang X & Qiu J, *J Power Sources*, 239 (2013) 81.

48 Hulicova-Jurcakova D, Seredych M, Lu G Q, Kodiweera N, Stallworth P E, Greenbaum S & Bandosz T J, *Carbon*, 47 (2009) 1576.

49 Puziy A M, Poddubnaya O I & Ziatdinov A M, *Appl Surf Sci*, 252 (2006) 8036.

50 Puziy A M, Poddubnaya O I, Martínez-Alonso A, Suárez-García F & Tascón J M D, *Carbon*, 40 (2002) 1493.

51 Kang K Y, Lee B I & Lee J S, *Carbon*, 47 (2009) 1171.

52 Wu D, Fu R, Dresselhaus M S & Dresselhaus G, *Carbon*, 44 (2006) 675.

53 Sankaran M & Viswanathan B, *Carbon*, 45 (2007) 1628.

54 Sankaran M, Muthukumar K & Viswanathan B, *Fullerenes, Nanotubes Carbon Nanostruct*, 13 (2005) 43.

55 Sankaran M & Viswanathan B, *Carbon*, 44 (2006) 2816.

56 Ou J, Zhang Y, Chen L, Yuan H & Xiao D, *RSC Adv*, 4 (2014) 63784.

57 Viswanathan B, Murugesan S, Ariharan A & Lakhi K S, *Adv Por Mater*, 1 (2013) 122.

58 Lee Y J & Radovic L R, *Carbon*, 41 (2003) 1987.

59 Zickler G A, Smarsly B, Gierlinger N, Peterlik H & Paris O, *Carbon*, 44 (2006) 3239.

60 Chaudhari N K, Song M Y & Yu J S, *Sci Rep*, 4 (2014) 10.

61 Wohlgemuth S A, White R J, Willinger M G, Titirici M M & Antonietti M, *Green Chem*, 14 (2012) 1515.

62 Fan X, Yu C, Ling Z, Yang J & Qiu J, *ACS Appl Mater Interfaces*, 5 (2013) 2104.

63 Puziy A M, Poddubnaya O I, Socha R P, Gurgul J & Wisniewski M, *Carbon*, 46 (2008) 2113.

64 Kurita E, Tomonaga Y, Matsumoto S, Ohno K & Matsuura H, *J Mol Struct*, 639 (2003) 53.

65 Wang Y, Alsmeyer D C & Mccreery R L, *Chem Mater*, 2 (1990) 557.

66 Fuge G M, May P W, Rosser K N, Pearce SRJ & Ashfold M N R, *Diamond Relat Mater*, 13 (2004) 1442.

67 Chu P K & Li L, *Mater Chem Phys*, 96 (2006) 253.

68 Chen L F, Zhang X D, Liang H W, Kong M, Guan Q F, Chen P, Wu Z-Y & Yu S-H, *ACS Nano*, 6 (2012) 7092.

69 Rusop M, Soga T & Jimbo T, *Sol Energy Mater Sol Cells*, 90 (2006) 3214.

70 Claeyssens F, Fuge G M, Allan N L, May P W & Ashfold M N R, *Dalton Trans*, 19 (2004) 3085.

71 Han J C, Liu A P, Zhu J Q, Tan M L & Wu H P, *Appl Phys A*, 88 (2007) 341.

72 Rosas J M, Bedia J, Rodríguez-Mirasol J & Cordero T, *Ind Eng Chem Res*, 47 (2008) 1288.

73 Kuo M T, May P W, Gunn A, Ashfold M N R & Wild R K, *Diamond Relat Mater*, 9 (2000) 1222.

74 Boudou J P, Parent P, Suárez-García F, Villar-Rodil S, Martínez-Alonso A & Tascón J M D, *Carbon*, 44 (2006) 2452.

75 Li R, Wei Z, Gou X & Xu W, *RSC Adv*, 3 (2013) 9978.

76 Liu Z, Peng F, Wang H, Yu H, Tan J & Zhu L, *Catal Commun*, 16 (2011) 35.

77 Chaudhari K N, Song M Y & Yu J S, *Small*, 10 (2014) 2625.